J Mater Sci: Mater Electron (2020) 31:22351–22364

Effect of doping on microstructure and optical properties of ternary structure of $Zn_{1-x-y}B_xC_yO$ (B=Cu, C=Co) nano thin films

Elif Asikuzun[1], Ozgur Ozturk[2], Rifki Terzioglu[3], Lutfi Arda[4], and Cabir Terzioglu[5,*]

[1] *Department of Metallurgical and Materials Engineering, Faculty of Engineering and Architecture, Kastamonu University, Kastamonu, Turkey*
[2] *Department of Electrical and Electronics Engineering, Faculty of Engineering and Architecture, Kastamonu University, Kastamonu, Turkey*
[3] *Department of Electrical Electronics Engineering, Faculty of Engineering, Bolu Abant Izzet Baysal University, 14280 Bolu, Turkey*
[4] *Department of Mechatronics Engineering, Faculty of Engineering and Natural Sciences, Bahcesehir University, Besiktas, 34349 Istanbul, Turkey*
[5] *Department of Physics, Faculty of Arts and Sciences, Abant Izzet Baysal University, 14280 Bolu, Turkey*

Received: 28 August 2020
Accepted: 21 October 2020
Published online: 6 November 2020

ABSTRACT

We report the results of an in depth study of optical and microstuctural properties of thin films of $Zn_{1-x-y}Cu_xCo_yO$ system (x = 0,00 and 0.02, y = 0.00, 0.01, 0.02, 0.03, 0.04. and 0.05) which are grown by the sol–gel method. We have performed differential thermal analysis, and thermo gravimetric analysis/difference thermogravimetric analysis, x-ray diffraction, scanning electron microscopy, energy dispersive spectrometer, atomic force microscopy and UV–VIS spectrophotometer experiments. We have found that all of the studied samples are in hexagonal wurtzite structure and oriented along the (002) direction with a very weak signal for the (101) reflection. We have also found that the lattice parameter c increases with doping. All the films showed wrinkle network structure with nano-sized crystals and the grain size was observed to decrease with increasing Co doping. The bandgap was found to decrease from 3.28 to 3.22 eV with doping. All the above results will be discussed in detail.

1 Introduction

The science of semiconductor nano thin film has an important place in the scientific and the technological research areas. Nano thin films are formed by coating of atoms or molecules of the required material on a substrate using different production techniques and are typically about 1 μm in thickness. The importance of coating and the synthesis of new materials for the microelectronics and optics applications have led to

Address correspondence to E-mail: terzioglu_c@ibu.edu.tr

https://doi.org/10.1007/s10854-020-04736-2

significant increase in nano thin film processing technologies [1–5]. Thin films have been utilized to increase material lifetime or to protect against the external factors in solar cells, optical and electronic circuits, and the memory portions of computers [6–8].

Nowadays the rapid change in the thin film materials creates new opportunities for the development of new processes, materials and technologies. Therefore many experiments are carried out to improve the desired properties of the films.

In recent years, the production of semiconductor thin film materials that are nanometer size has a significant point of interest. Nano-crystal semiconductor materials that are in thin film format allow to improve the characteristic properties of materials. A gradual transition is observed to molecular structure from rigid structure due to the increasing number of particle that forms the material in this type materials.

Semiconductor nano thin films are divided into three main groups depending on the reduction of structural perfection degrees: (i) single layer single crystal films (homo epitaxial) that are deposited on the single crystal of the same material, (ii) multi-layer single crystal films which are obtained by depositing material A on single crystal material B, (iii) polycrystalline films that are grown on the amorphous substrates such as glass or quartz. Polycrystalline films, which can be grown by various simple methods [9], are semiconducting materials that are deposited on substrates such as metal, glass, ceramic and granite. This type of films has many applications, such as solar cell, semiconductor photodetectors and diodes. For these applications, especially in recent years, semiconductor films (ZnO, TiO2, NiO, etc.) have been doped with transition metals (Cu, Co, Mn, Ni, Fe, etc.) and rare earth elements (Yb, Er, Ho, Gd, Y, etc.) to enhance the structural, electrical, optical and the magnetic properties [10–15].

The Cu and Co doping in ZnO thin films have been intensively studied because of the magnetism of Co thin film at room temperature and the effect of Cu at deep acceptor level as well as a p-type semiconductor based on the oxidation states of Zn [16, 17]. There are some crucial questions, namely, whether the final nano material is a single phase of Cu/Co-doped ZnO or not and the Co/Cu ions are incorporated substitutionally for Zn^{+2} or interstitially with uniform distribution or clusters keeping the ZnO structure [18].

In our earlier works [16, 17, 19, 20], we have reported that Co replaces Zn substitutionally yielding ZnCoO single phase for $Zn_{1-x}Co_xO$ up to $x \leq 0.12$. The adding of a small amount of Cu and Co into ZnO

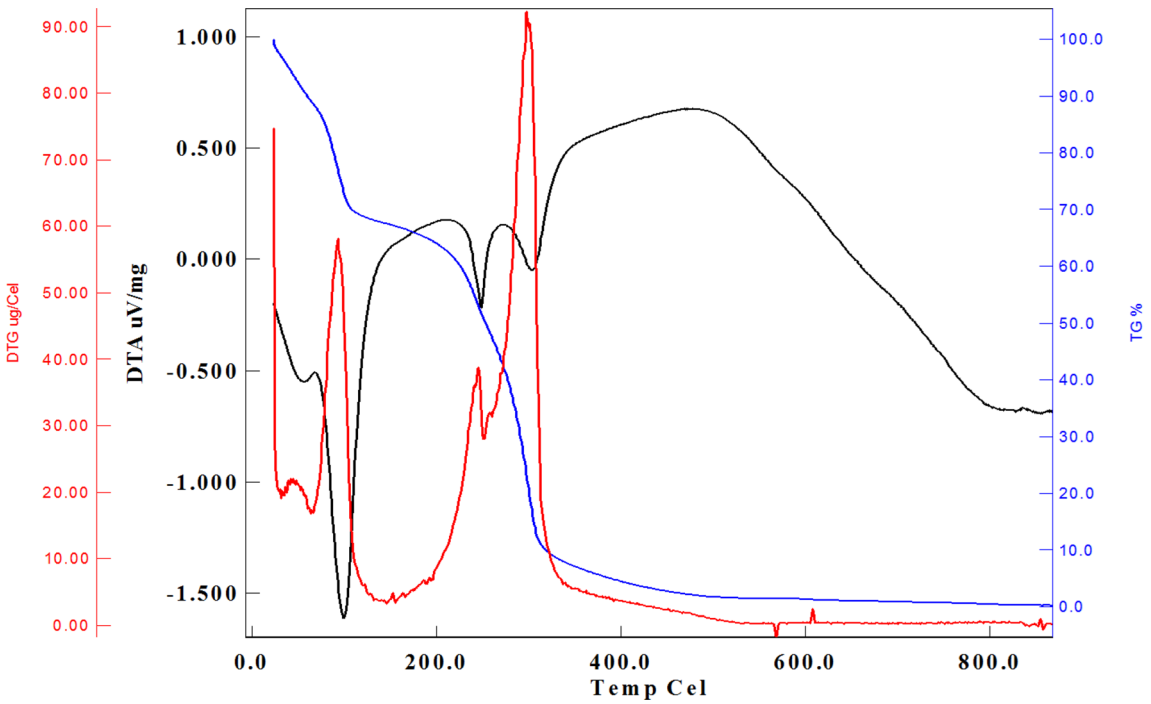

Fig. 1 The investigation of possible weight loss and the thermal behavior of $Zn_{0.93}Cu_{0.02}Co_{0.05}O$ sample with DTA and TGA measurements

helps to produce industrially accepted enriched thin films [10, 19, 21].

Hsu et al. [22] examined, methodically, the effect of annealing on the structural and the magnetic properties for Co-doped ZnO films under air, Ar, and Ar/H_2 atmospheres at 523 K and concluded that there is a strong correlation between the oxygen vacancies in the ZnO lattice and the ferromagnetism of the films. Khare et al. [23] found that, after annealing at 673 K, the magnetization of annealed $Zn_{0.98}Co_{0.02}O$ films was unrelated to the reductive or oxidizing atmosphere.

The aims of this study are to analyze characterization and processing parameters of $Zn_{1-x-y}Cu_xCo_yO$ (x = 0,00 and 0.02, y = 0.00, 0.01, 0.02, 0.03, 0.04 and 0.05) thin films, to produce c-axis oriented and single phase $Zn_{1-x-y}Cu_xCo_yO$ thin films, and to examine doping effect on the micro-structural and optical properties of $Zn_{1-x-y}Cu_xCo_yO$ thin films.

2 Experimental details

$Zn_{1-x-y}Cu_xCo_yO$ compounds are manufactured at different x and y ranges (x = 0,00 and 0.02 and, y = 0.00, 0.01, 0.02, 0.03, 0.04 and 0.05) using the sol–gel method. Zn acetate dihydrate, cobalt acetate tetrahydrate and copper acetate tetrahydrate are used as precursors. To prepare a homogeneous solution and to improve the adhesion on the glass substrate, methanol and acetyl acetone are used as the solvent. The solution is stirred until a clear solution is obtained using a temperature controlled magnetic stirrer at 60 °C for 8 h. Using the dip-coating method in the vertical furnace, the glass substrates were covered with solutions at 400 °C for 2 min. Coated nano thin films were cooled for 3 min between the dips. To get a dense and homogeneous coating the process was repeated 10 times. Afterwards, all samples were annealed at 600 °C for 30 min for nano bulk materials using the muffle furnace.

3 Results and discussion

The prime novelty of this research is the production of c-axis oriented and single phase $Zn_{1-x-y}Cu_xCo_yO$ thin films. In addition, the goals of the present work are the analyses of characterization and processing parameters of $Zn_{1-x-y}Cu_xCo_yO$ (x = 0,00 and 0.02, y = 0.00, 0.01, 0.02, 0.03, 0.04 and 0.05) thin films and the examination of doping effect on the micro-structural and optical properties of $Zn_{1-x-y}Cu_xCo_yO$ thin films.

3.1 XRD and TGA/DTA measurements

The thermal behavior of $Zn_{1-x-y}Cu_xCo_yO$ samples, which were produced by the sol–gel technique dried at room temperature for 3 days, was investigated using the Differential Thermal Analysis (DTA) and Thermo Gravimetric Analysis/Difference Thermogravimetric Analysis (TGA/DTG) techniques. Figure 1 shows the TGA/DTG and DTA curves of

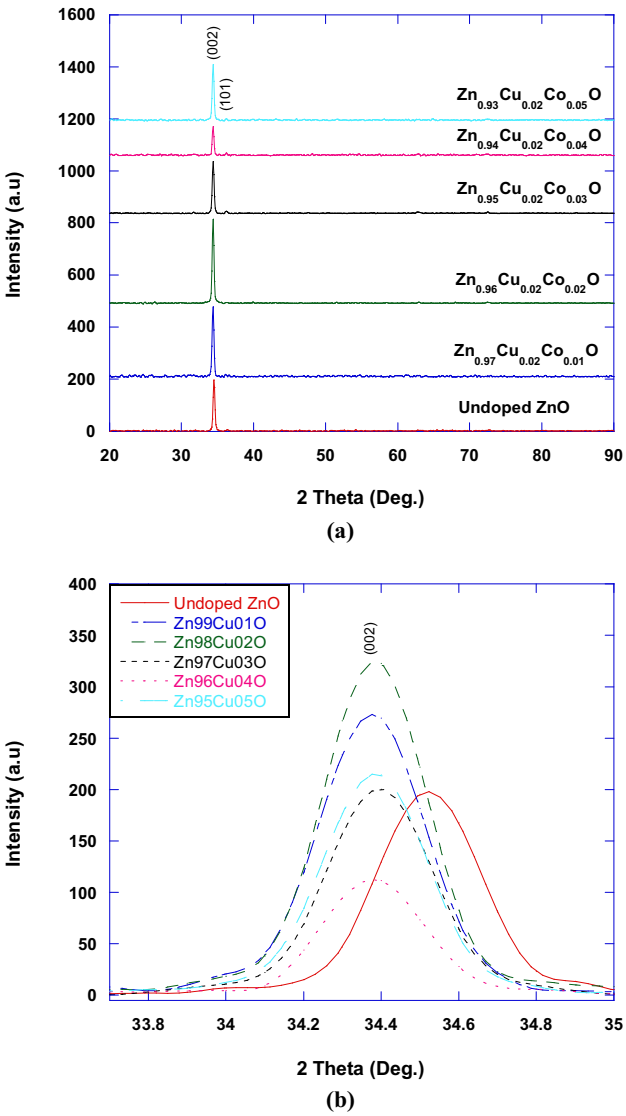

Fig. 2 XRD patterns of $Zn_{1-x-y}Cu_xCo_yO$ nano thin film materials

Table 1 Some structural values ZnO and Cu/Co doped ZnO nano thin films

Samples	*c* (002)	*a* (101)	FWHM (deg.)	Grain size (nm)	*F*	*L* (nm)	α (°)	β (°)	$\sigma*10^8$ (N/m^2)
Undoped ZnO	5.18	–	0.256	31.73	1.000	1.29	90	120	− 17.5
$Zn_{0.97}Cu_{0.02}Co_{0.01}O$	5.19	–	0.245	33.13	0.982	1.29	90	120	− 9.63
$Zn_{0.96}Cu_{0.02}Co_{0.02}O$	5.20	–	0.258	32.51	1.014	1.30	90	120	− 7.26
$Zn_{0.95}Cu_{0.02}Co_{0.03}O$	5.21	3.24	0.269	30.19	1.042	0.62	108	110	1.67
$Zn_{0.94}Cu_{0.02}Co_{0.04}O$	5.20	3.24	0.292	27.85	1.055	0.62	108	110	− 1.04
$Zn_{0.93}Cu_{0.02}Co_{0.05}O$	5.20	3.25	0.372	21.86	1.082	0.62	108	110	− 7.34

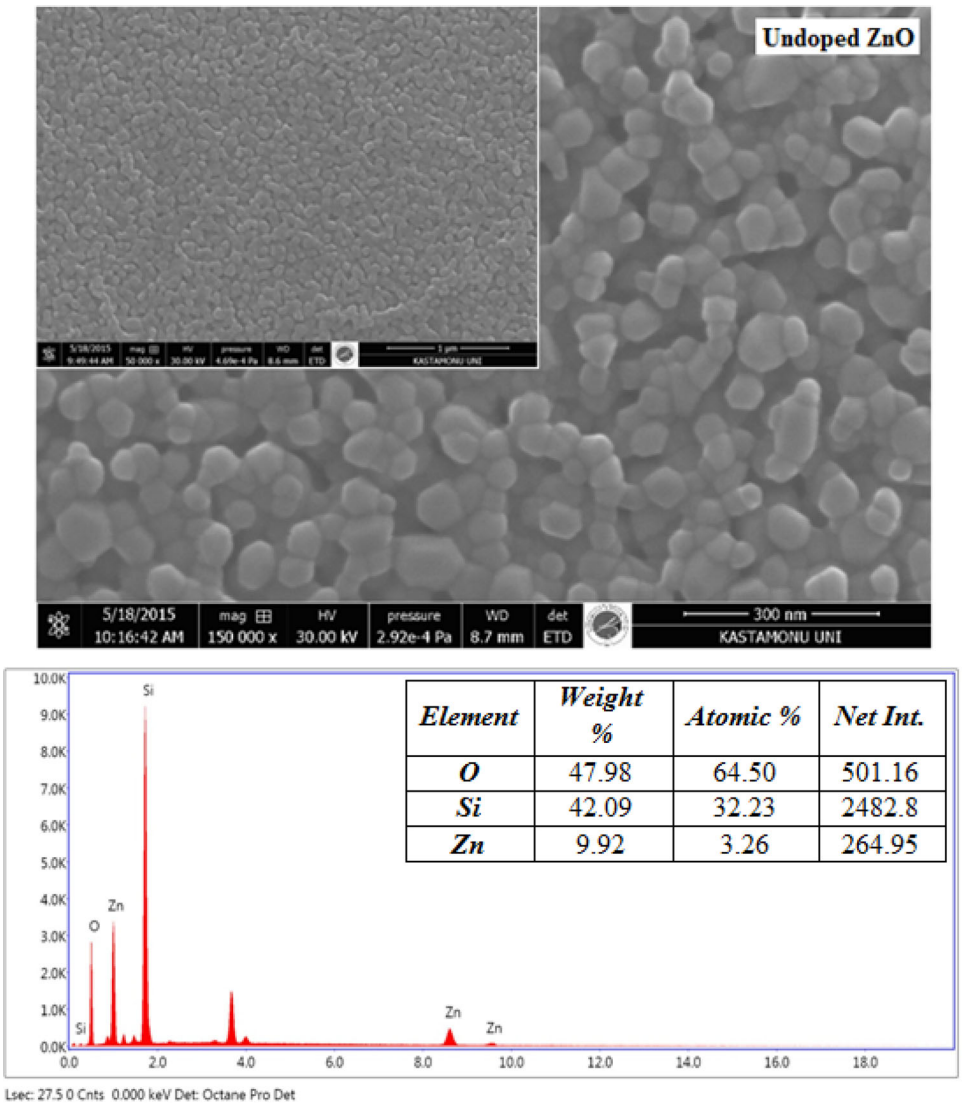

Fig. 3 SEM and EDS images of undoped ZnO nano thin film material

$Zn_{0.93}Cu_{0.}02Co_{0.05}O$ sample in the temperature range 25–1000 °C with a heating rate of 10 °C/min.

As can be seen from Fig. 1, the first weight loss (32%) depending on evaporation of water and the removal of solvent can be found at 100 °C and a strong endothermicity is obvious around the same temperature. A wide exothermic peak follows in the DTA curve until 210 °C temperature is reached in this region, the residual solvent evaporates (12%) (see, Fig. 1 TGA curve). It could also be deduced from the figure that the DTG (measuring the weight loss of $Zn_{0.93}Cu_{0.02}Co_{0.05}O$ sample) curve decreases

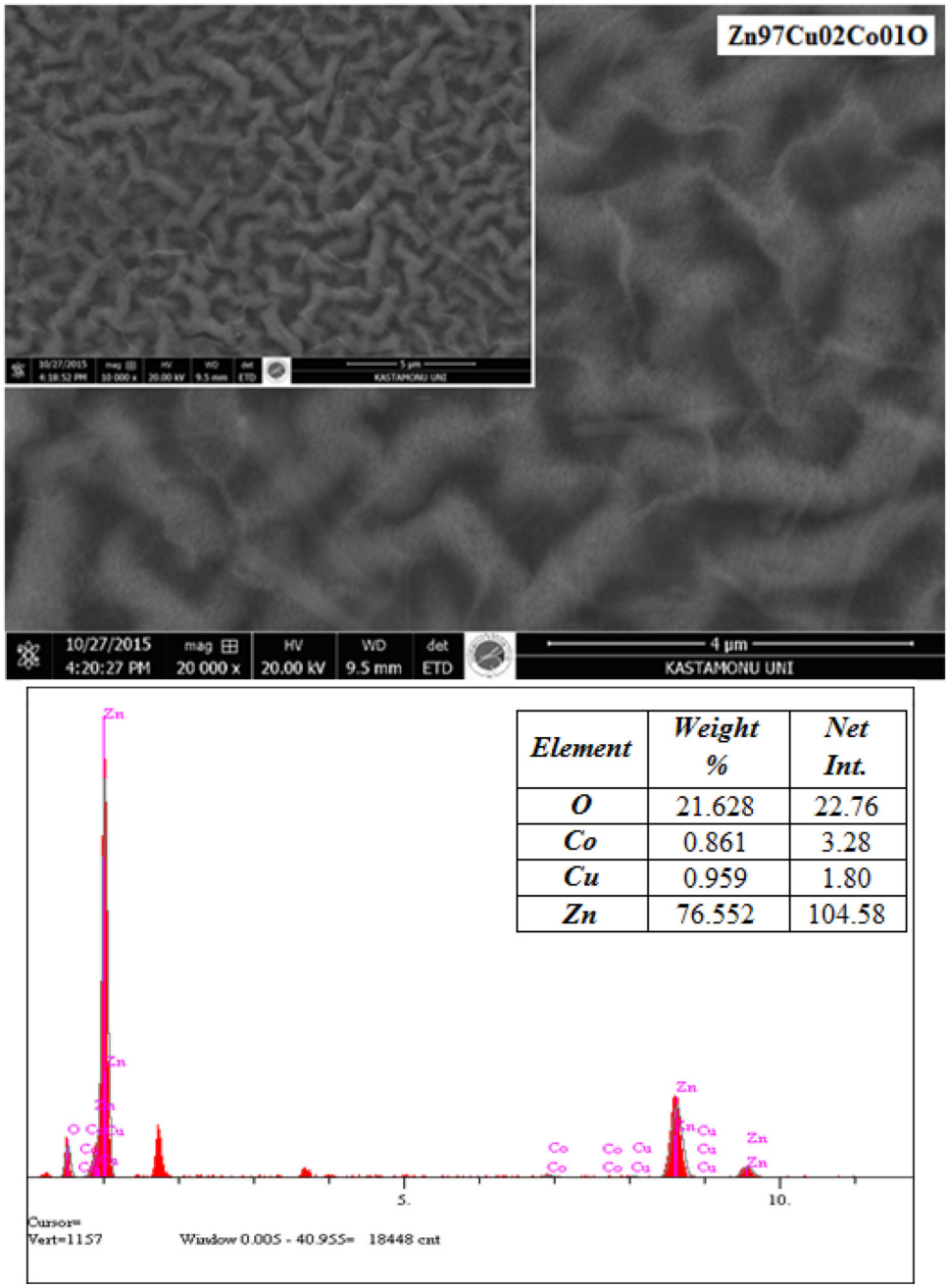

Fig. 4 SEM and EDS images of $Zn_{0.97}Cu_{0.02}Co_{0.01}O$ nano thin film material

when exothermic reaction occurs. A 48% sudden and sharp mass loss occurred between 210 and 330 °C due to the evaporation of the volatile organic components. The remaining organic materials are found to burn out until 600 °C which is preceded with two small endothermic signals around 330 °C. A further 8% weight loss in TGA data can be seen in the 330–600 °C region.

X-ray diffraction (XRD) analysis were performed on the Cu and Co doped samples of ZnO nano thin films and are shown in Fig. 2. All of the studied samples are found to be in hexagonal wurtzite structure and are oriented along the (002) direction with a very weak signal for the (101) reflection. As seen from Fig. 2, no secondary phase of CuO or CoO was observed which means Co^{+2} and Cu^{+2} ions replace the Zn^{+2} ions of the ZnO host semiconductor without changing the original wurtzite structure. Since the ionic radius of Zn^{+2} (0.74 Å) is larger than the ionic radius of Co^{+2} (0.70 Å) and Cu^{+2} (0.73 Å)

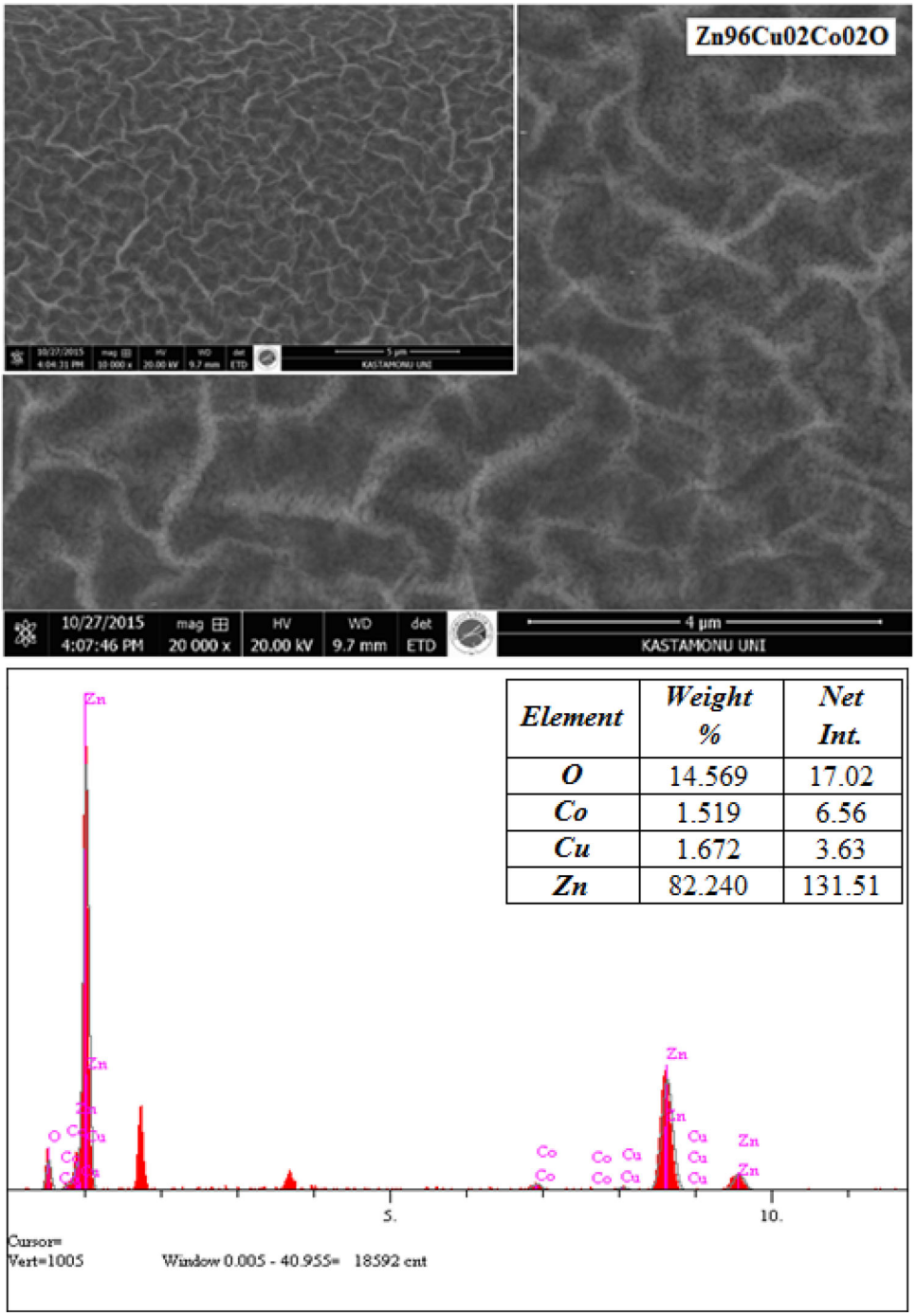

Fig. 5 SEM and EDS images of $Zn_{0.96}Cu_{0.02}Co_{0.02}O$ nano thin film material

this is an expected result.[24]. It can also be seen that as the doping concentration is increased, the (002) peak shifts to the lower angles compared to that of the undoped ZnO film (34.46°) and its intensity increases. Also, the lattice parameter *c* is found to increase with doping which indicates that the dopant ions substitute into the Zn^{+2} sites.

These results are supported with calculation of the degree of orientation (Table 1). The change of orientation is led to changes of the bond angles α and β. Values of α which is 90° for hexagonal wurtzite ZnO structure are 108° for $Zn_{0.95}Cu_{0.02}Co_{0.03}O$, $Zn_{0.94}Cu_{0.02}Co_{0.04}O$ and $Zn_{0.93}Cu_{0.02}Co_{0.05}O$, respectively. The values of β which are 120° for hexagonal wurtzite ZnO structure are 110°.

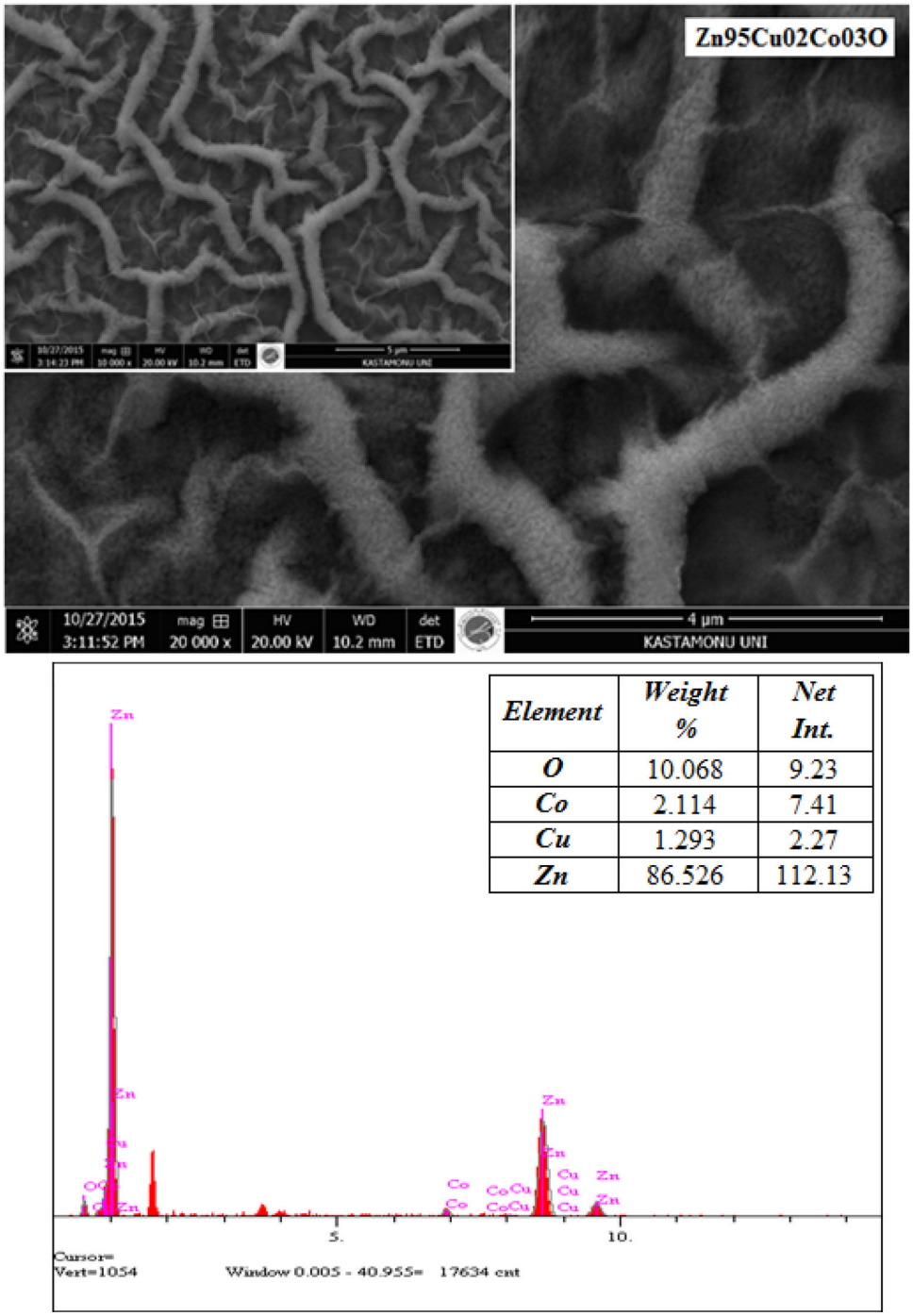

Fig. 6 SEM and EDS images of $Zn_{0.95}Cu_{0.02}Co_{0.03}O$ nano thin film material

In doped films, the FWHM value of the (002) peak is larger than the one in undoped ZnO film. These results show that the Cu/Co doped ZnO films have better crystal size than undoped ZnO nano thin film which is proved by the orientation of degree calculation [24]. Degree of orientation of (002) plane increases with increasing Cu/Co doping. It can be clearly said that the degree of orientation is influenced by the Cu/Co doping. In addition, the values of bond length (L) (see Table 1) increased with decreasing the Cu/Co fraction. Lattice parameters *a* and *c* increase with doping compared with undoped ZnO.

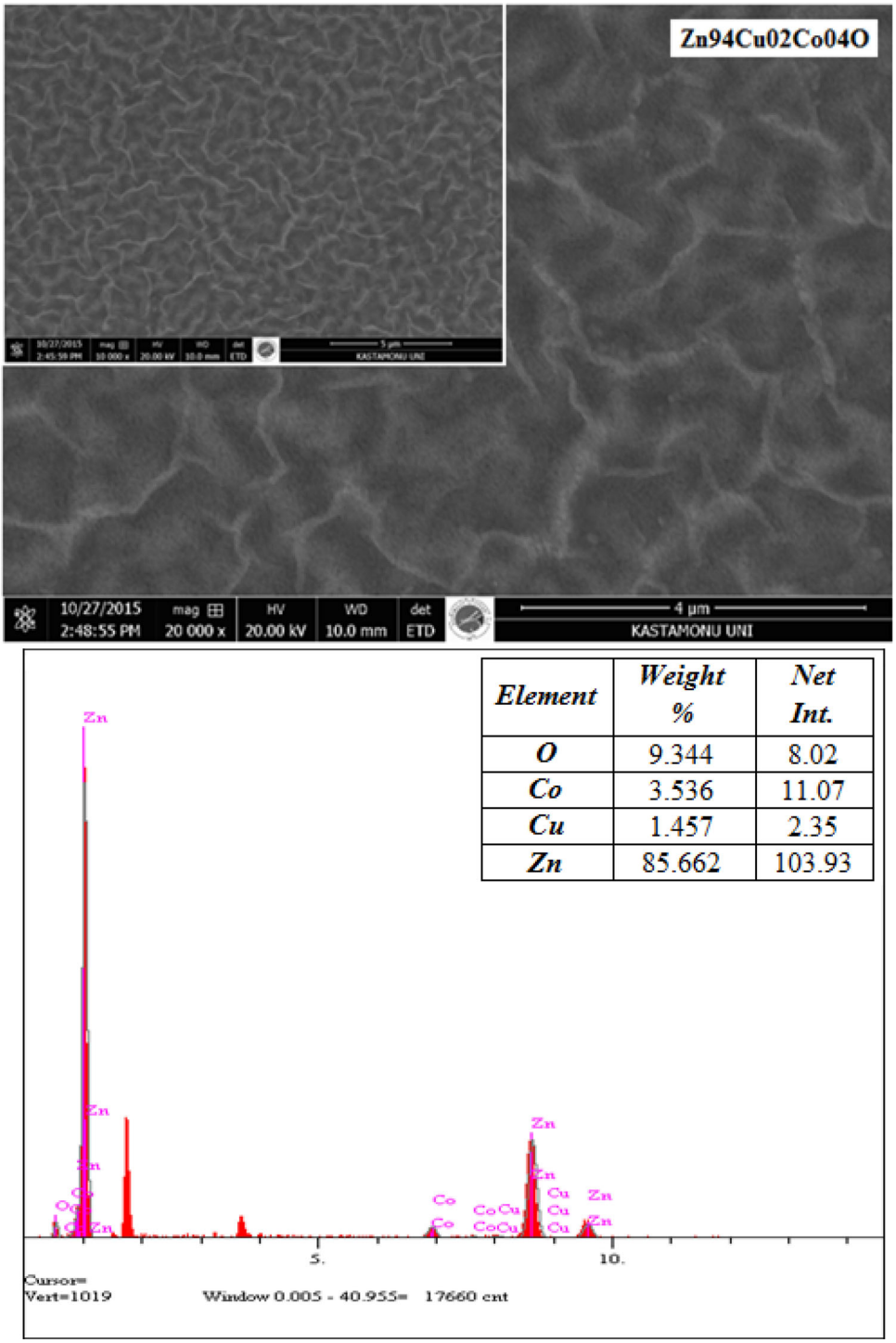

Fig. 7 SEM and EDS images of $Zn_{0.94}Cu_{0.02}Co_{0.04}O$ nano thin film material

3.2 SEM–EDS measurements

Scanning electron microscopy (SEM) images of undoped and Co doped ZnO films are shown in Figs. 3, 4, 5, 6, 7 and 8. According to the SEM results, films exhibit wrinkle network structure with nano-sized crystals. The results indicate that the surface morphology changes with Co doping. Wrinkle structure does not change with the increasing Co doping, but grain sizes change to denser structure form. The average grain size of the films is 29.108 nm. Increasing Co doping leads to smaller grains which show that Co inhibits growth of the ZnO lattice. The reduction in grain size with Co doping might be due

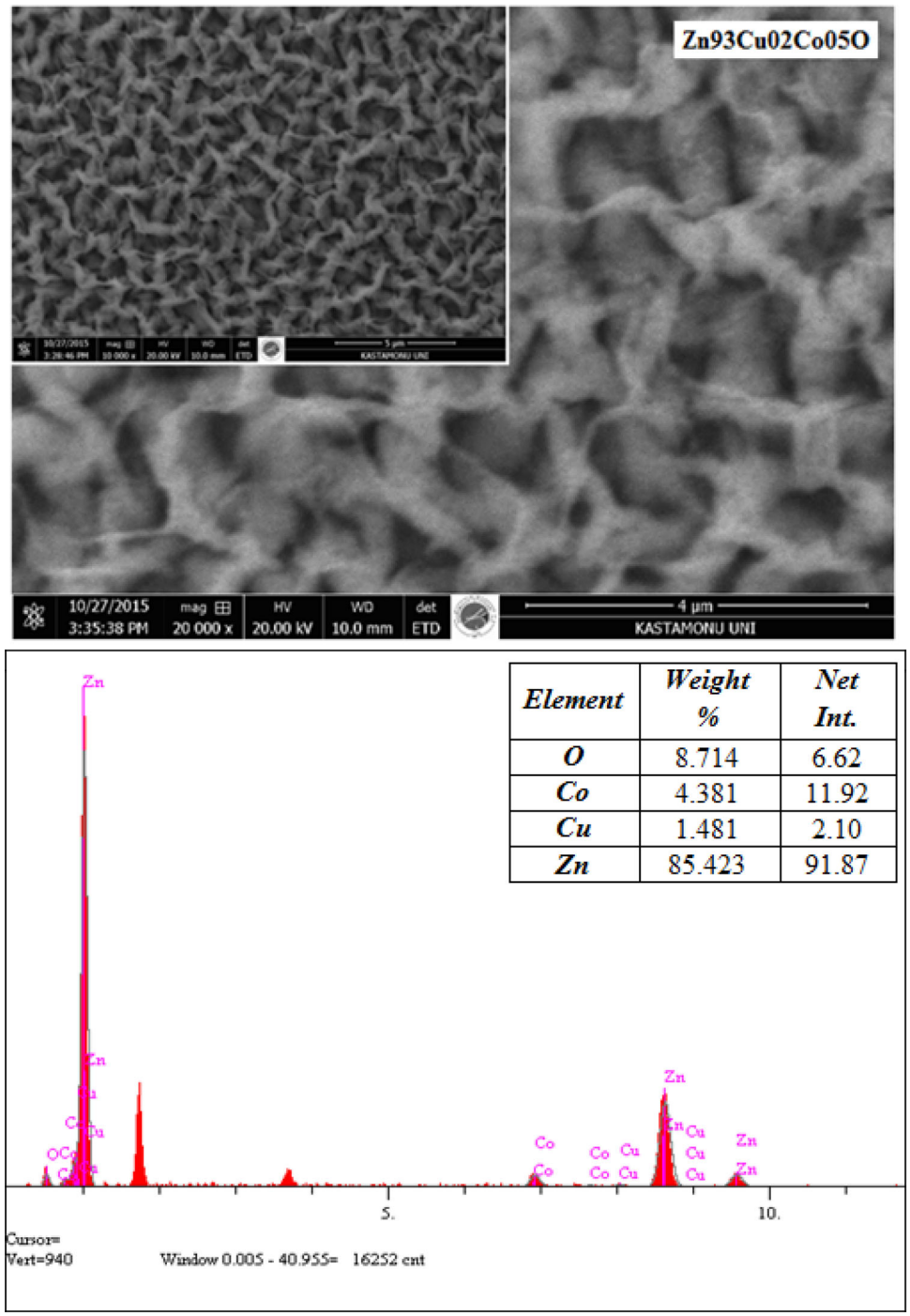

Fig. 8 SEM and EDS images of $Zn_{0.93}Cu_{0.02}Co_{0.05}O$ nano thin film material

to pinning and dragging effects of the dopant at and between the grain boundaries, respectively. These two effects can also be seen to be in action in the observed mobility decrease in the grain boundaries.

Chemical purity and stoichiometries of the nano thin film samples are analyzed by the Energy Dispersive Spectrometer (EDS) measurements. Weight, atomic percentage, and intensity of compositional elements such as O, Cu, Co and Zn are given in Figs. 3, 4, 5, 6, 7 and 8. In addition, the presence oxygen is low in $Zn_{0.93}Cu_{0.02}Co_{0.05}O$ nano thin film. This behavior observed that existence of defects is lower in this film.

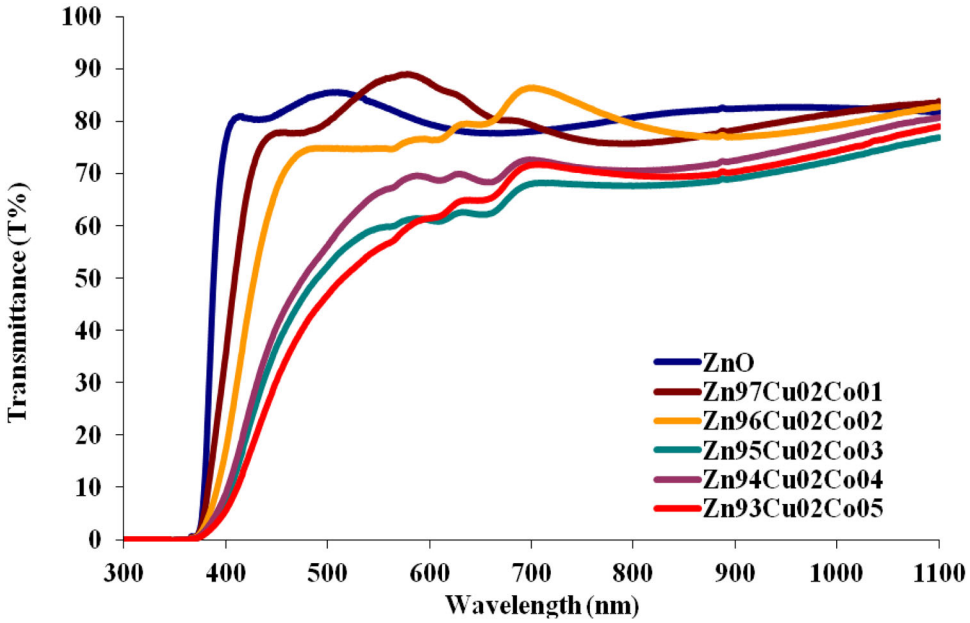

Fig. 9 Optical transmittance spectra of all ZnO nano thin films

Table 2 Average transmittance, Energy Gap (E_g), Urbach energy (E_u) and steepness parameter and values for ZnO and Cu/Co doped ZnO nano thin films

Samples	Average transmittance (%)[a]	Energy gap (eV)	E_U (meV)[b]	Steepness parameter $\beta*10^{-1}$
Undoped ZnO	81.12	3.28	98.10	2.63
$Zn_{0.97}Cu_{0.02}Co_{0.01}O$	77.79	3.27	160.77	1.62
$Zn_{0.96}Cu_{0.02}Co_{0.02}O$	73.57	3.25	225.22	1.14
$Zn_{0.95}Cu_{0.02}Co_{0.03}O$	67.22	3.24	298.50	0.86
$Zn_{0.94}Cu_{0.02}Co_{0.04}O$	59.82	3.23	300.30	0.86
$Zn_{0.93}Cu_{0.02}Co_{0.05}O$	57.26	3.22	333.33	0.77

[a]The average transmittance values are calculated from the transmittance data of wavelength from 400 to 700 nm

[b]$k_b = 8.617 \times 10^{-2}$ meV/K and $T = 300$ K

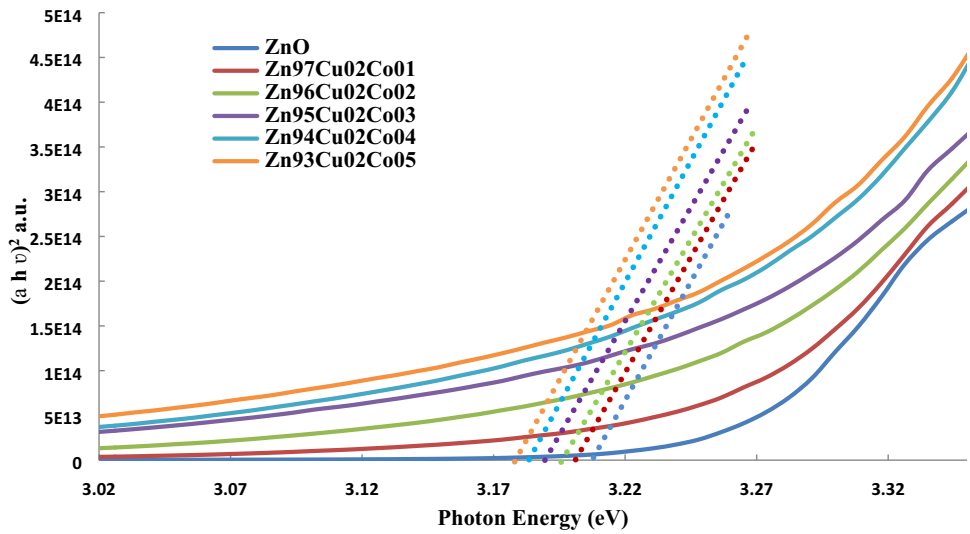

Fig. 10 The plots of $(\alpha h\nu)^2$ versus $(h\nu)$ for ZnO and ZnCuCoO nano thin films

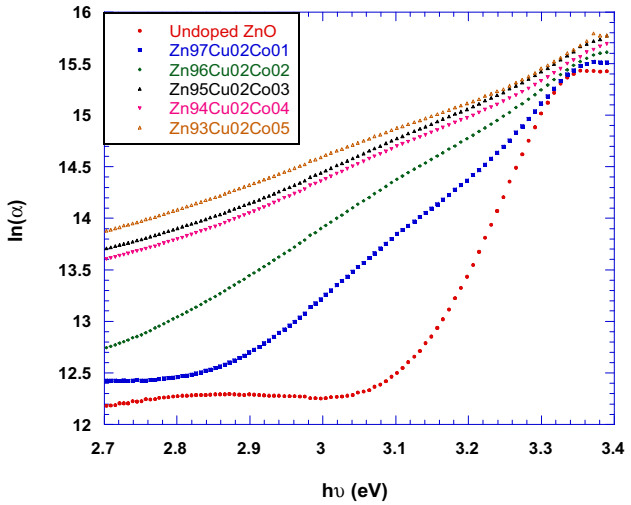

Fig. 11 The Urbach plots of the ZnCuO:Co nano thin films

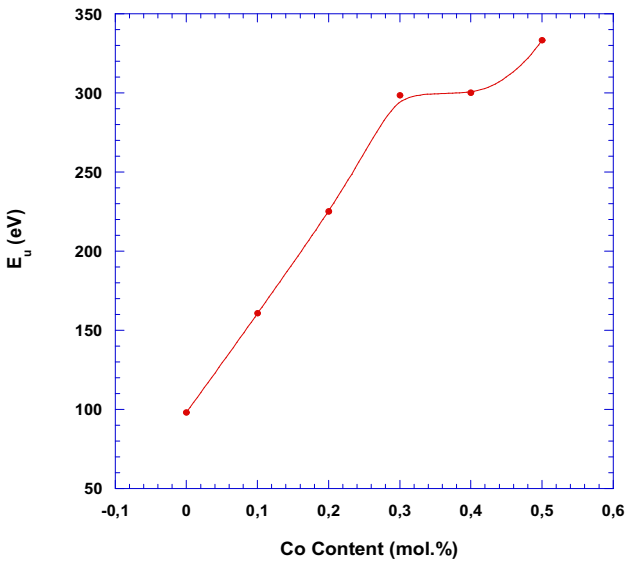

Fig. 12 Variations of Urbach energies and steepness parameter as a function of Co content

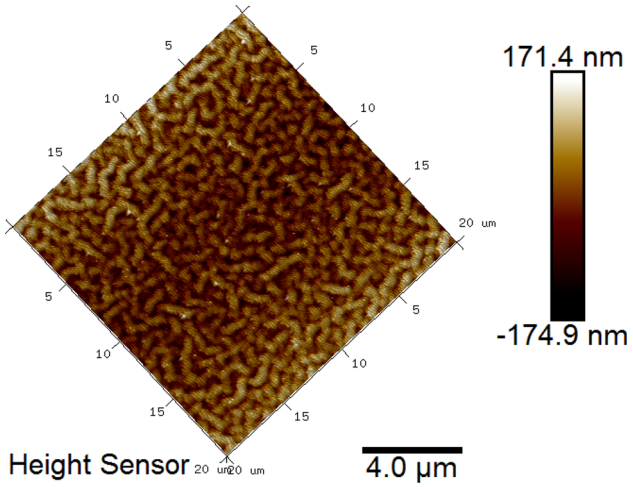

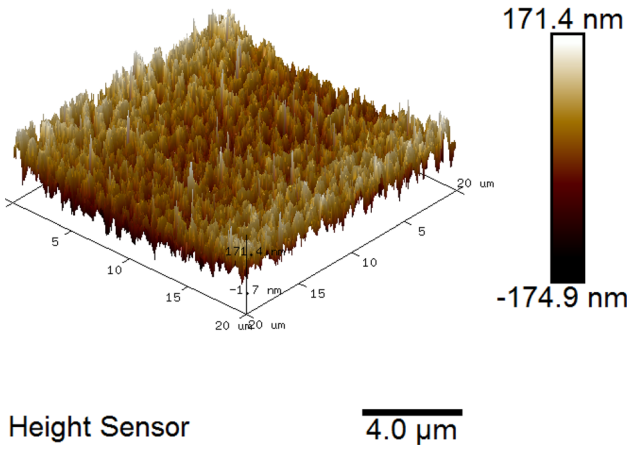

Fig. 13 AFM analyses of $Zn_{0.93}Cu_{0.02}Co_{0.05}O$ nano thin film materials

3.3 Optical measurements

Figure 9 displays the optical transmission spectrum of the Cu/Co doped ZnO nano thin films in the wavelength range (360–450) nm. Cu–Co doping is seen to lead to a significant shift in the absorption edge. The optical transmittance of pure ZnO film has an absorption edge at around 405 nm and is approximately equal to 81% at that wavelength (Table 2). The average transmittance values of Cu/Co doped ZnO nano thin films are under 80% and their transmittances are smaller than that of ZnO thin film [25]. For the ZnO film, the optical band gap is approximately 3.28 eV which is in agreement with the literature data, and is found to be in 3.22–3.27 eV range for the Cu/Co doped samples which are displayed in Fig. 10 and Table 2. They indicate that Cu/Co doping reduces the band gap and increases the band-tail width (Fig. 11). As can be seen from Table 2, Urbach energy (E_u) tends to increase with increasing Cu/Co doping (Fig. 12). The steepness parameter decreases with the increasing Urbach energy [26].

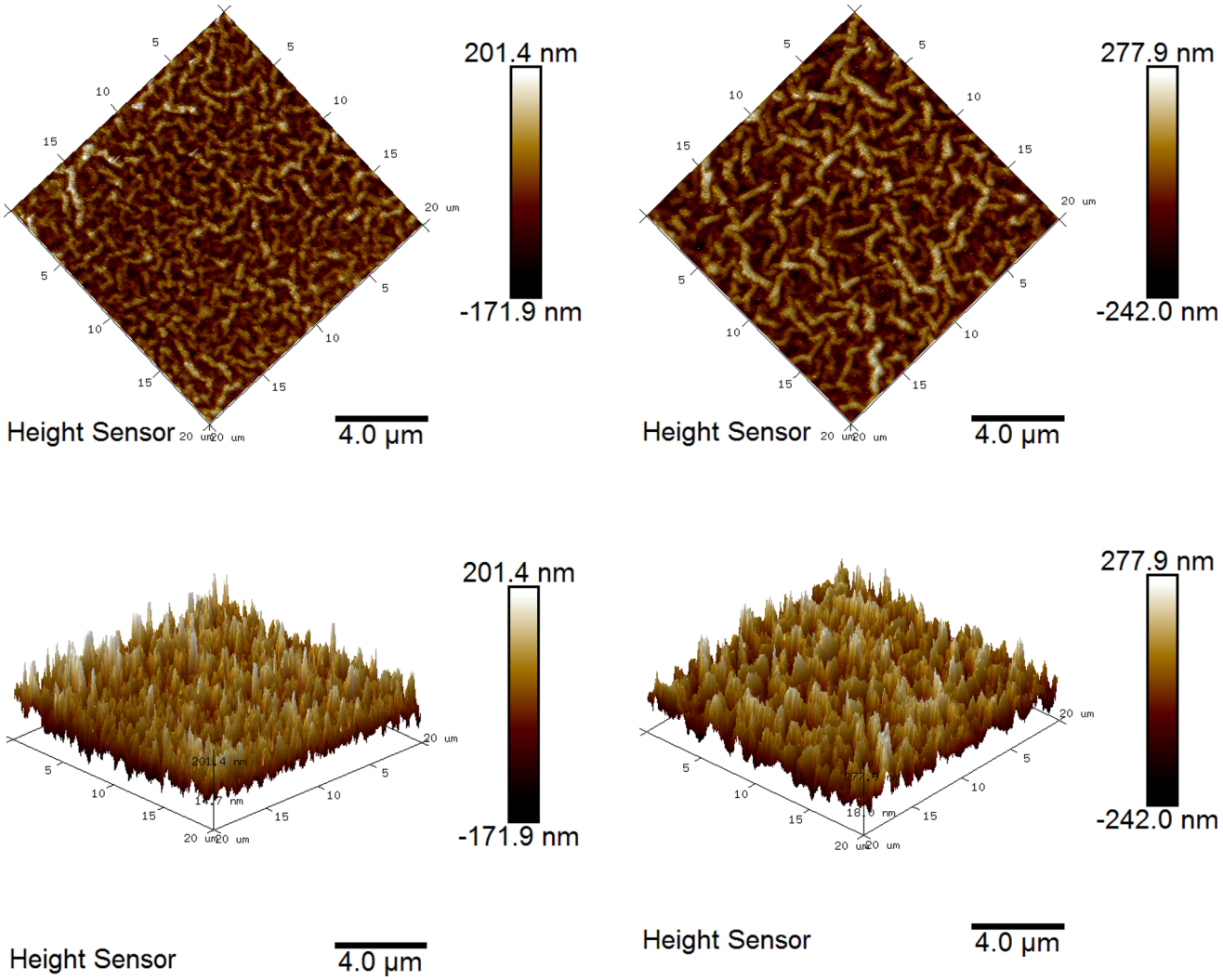

Fig. 14 AFM analyses of $Zn_{0.94}Cu_{0.02}Co_{0.04}O$ nano thin film materials

Fig. 15 AFM analyses of $Zn_{0.95}Cu_{0.02}Co_{0.03}O$ nano thin film materials

3.4 AFM measurements

Figures 13, 14, 15, 16 and 17 (20 × 20 μm) exhibit the 2D and 3D views of the surface morphology of Cu/Co doped ZnO-based semiconductor nano thin films. As seen from these Atomic Force Microscopy (AFM) images, surface morphology of nano thin films changes with increasing Cu/Co doping. Surface roughness is found to increase with Co doping. Surface roughness is found to increase with Co doping. While the film surface of Co0.01 sample that has the minimum doping amount is smoother, the film surface of Co0.05 that has maximum doping amount is rougher [27, 28]. Surface flatness significantly affects the transmittance of the ZnO-based nano thin films which might be due to light scattering and reflection from the rough surface (Fig. 9).

4 Conclusions

We have presented a study of Cu and Co doping on the stuctural and optical properties of ZnO thin films. The main findings of the study can be summarized as follows:

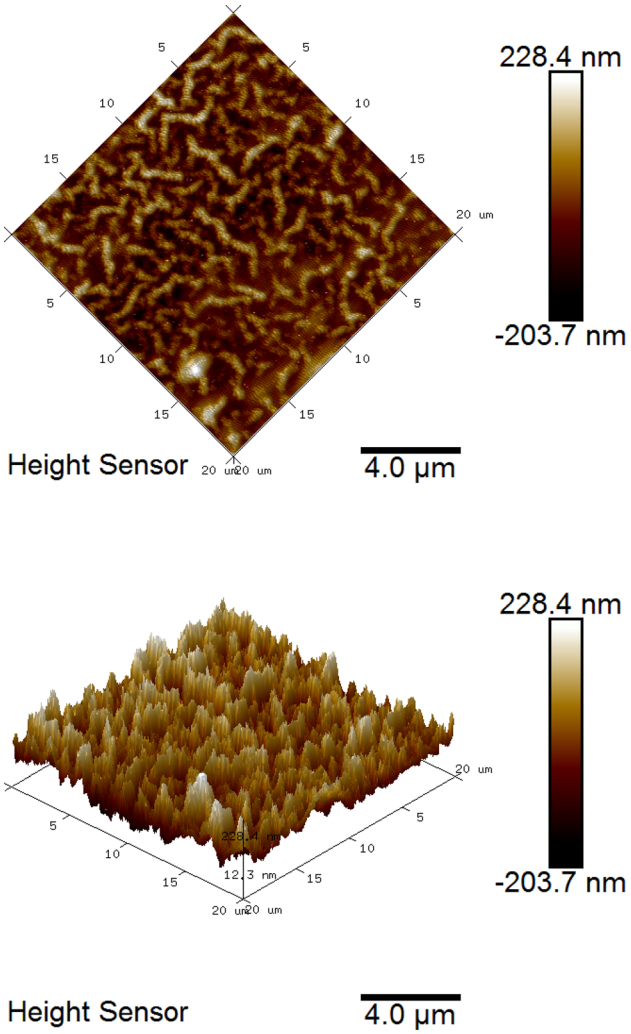

Fig. 16 AFM analyses of $Zn_{0.96}Cu_{0.02}Co_{0.02}O$ nano thin film materials

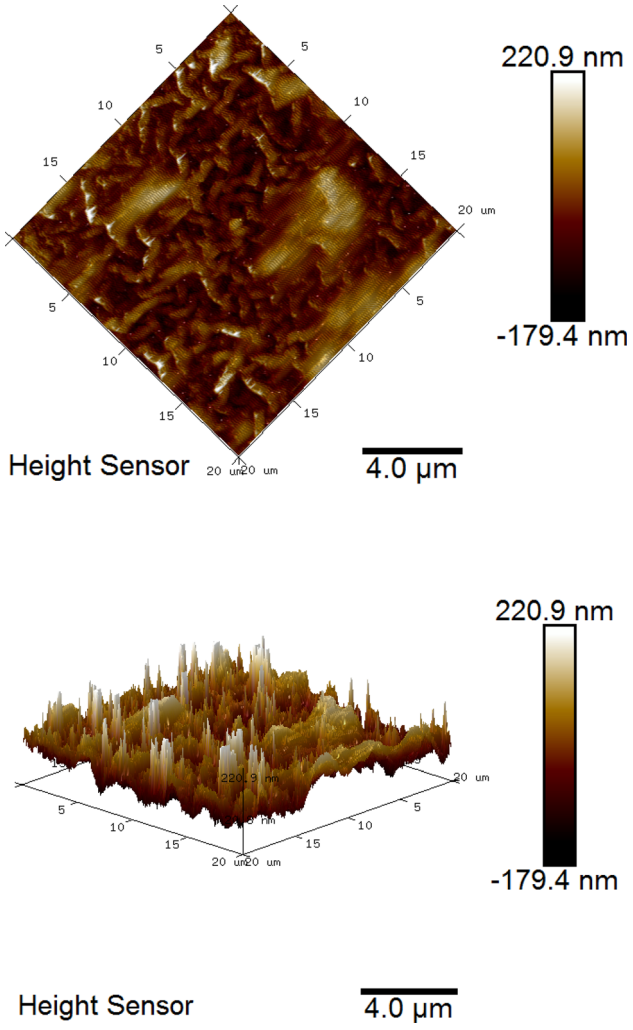

Fig. 17 AFM analyses of $Zn_{0.97}Cu_{0.02}Co_{0.01}O$ nano thin film materials

All samples in the present study were found to be oriented along the (002) direction with a small reflection from (101) and have a hexagonal wurtzite type structure. No secondary CuO and/or CoO phases were observed. We have measured the optical transmission of the samples in the $360-450nm$ wavelength range and found that Cu–Co doping decreases the band gap up to 60 meV. Co/Cu doping shifts the absorption edge significantly and leads to a decrease in the transmittance of the films. For Cu/Co doped nano thin films, the optical band gap energy range is between 3.22 and 3.27 eV. Band gap energy of the Cu/Co doped ZnO nano thin films is smaller than that of the ZnO nano thin film. According to the AFM images, surface morphology of nano thin films changes with increasing Cu/Co doping. While the film surface of $Zn_{0.97}Cu_{0.02}Co_{0.01}O$ sample that has the minimum doping amount is smoother, the film surface of $Zn_{0.93}Cu_{0.02}Co_{0.05}O$ which has maximum doping amount is the roughest.

References

1. Z. Fan, J.G. Lu, J. Nanosci. Nanotechnol. **5**, 1561–1573 (2005)
2. E. Asikuzun, O. Ozturk, L. Arda, D. Akcan, S.D. Senol, C. Terzioglu, J. Mater. Sci. **26**, 8147–8159 (2015)
3. Y. Caglar, M. Caglar, S. Ilican, Curr. Appl. Phys. **12**, 963–968 (2012)
4. C. Wagner, W. Schottky, Z. Phys, Chem. B. **11**, 163–210 (1930)

5. B.C. Steele, *Electronic Ceramics* (Springer, New York, 1991)
6. L. Eckertova, *Physics of Nano Thin Films* -, 2nd edn. (Plenum Press, New York, 1986)
7. J.L. Snoek, Philos. Tech. Rev. **8**, 353–360 (1946)
8. G. Destriau, Philos. Mag. **38**, 700–739 (1947)
9. S.M. Sze, *Physics of Semiconductor Devices*-, 2nd edn. (Wiley, Hoboken, 1981)
10. E. Asikuzun, O. Ozturk, L. Arda, C. Terzioglu, J. Mol. Struct. **1165**, 1–7 (1981)
11. D.J. Hagen, T.S. Tripathi, I. Terasaki, M. Karppinen, Semicond. Sci. Technol. **33**, 115015 (2018)
12. E. Asikuzun, O. Ozturk, L. Arda, C. Terzioglu, J. Mater. Sci. **28**, 14314–14322 (2017)
13. E. Asikuzun, A. Donmez, L. Arda, O. Cakiroglu, O. Ozturk, D. Akcan, C. Terzioglu, Ceram. Int. **41**, 6326–6334 (2015)
14. D. Kumar, P. Mandal, A. Singh, C. Pant, J. Mater. Res. **33**, 4165–4172 (2018)
15. S. Ozharar, D. Akcan, L. Arda, J. Optoelect. Adv. Mater. **18**, 65–69 (2016)
16. K.S.S. Ali, R. Saravanan, S. Israel, M. Açikgöz, L. Arda, Phys. B **405**, 1763–1769 (2010)
17. L. Arda, M. Acikgoz, N. Dogan, D. Akcan, O. Cakiroglu, J. Supercond. Novel Magn. **27**, 799–804 (2014)
18. Z.K. Heiba, L. Arda, M.B. Mohamed, N.Y. Mostafa, N. Dogan, J. Supercond. Novel Magn. **26**, 3487–3493 (2013)
19. Z.K. Heiba, L. Arda, J. Mol. Struct. **1022**, 167–171 (2012)
20. E. Asikuzun, A. Donmez, L. Arda, O. Cakıroglu, O. Ozturk, D. Akcan, M. Tosun, S. Ataoglu, C. Terzioglu, Ceram. Int. **41**, 6326–6334 (2015)
21. T.S. Herng, S.P. Laua, S.F. Yu, H.Y. Yang, X.H. Ji, J. Appl. Phys. **99**, 086101 (2006)
22. H.S. Hsu, J.C.A. Huang, Y.H. Huang, Y.F. Liao, M.Z. Lin, C.H. Lee, J.F. Lee, S.F. Chen, L.Y. Lai, C.P. Liu, Appl. Phys. Lett. **88**, 242507 (2006)
23. N. Khare, M.J. Kappers, M. Wei, M.G. Blamire, J.L. Manus-Driscoll, Adv. Mater. **18**, 1449 (2006)
24. E. Asikuzun, O. Ozturk, L. Arda, A.T. Tasci, F. Kartal, C. Terzioglu, Ceram. Int. **42**, 8085–8091 (2016)
25. R.C. Rai, J. Appl. Phys. **113**, 153508 (2013)
26. S. Ilican, M. Caglar, Y. Caglar, Appl. Surf. Sci. **256**, 7204–7210 (2010)
27. C.Y. Tsay, K.S. Fan, Y.W. Wang, C.J. Chang, Y.K. Tseng, C.K. Lin, Ceram. Int. **36**, 1791–1795 (2010)
28. C.Y. Tsay, W.C. Lee, Curr. Appl. Phys. **13**, 60–65 (2013)